J Sci Comput (2016) 68:826–847
DOI 10.1007/s10915-015-0160-y

A Hybridized Discontinuous Galerkin Method for 2D Fractional Convection–Diffusion Equations

Shuqin Wang[1,2] · **Jinyun Yuan**[2] · **Weihua Deng**[1] · **Yujiang Wu**[1]

Received: 23 June 2015 / Revised: 16 November 2015 / Accepted: 28 December 2015 /
Published online: 18 January 2016

Abstract A hybridized discontinuous Galerkin method is proposed for solving 2D fractional convection–diffusion equations containing derivatives of fractional order in space on a finite domain. The Riemann–Liouville derivative is used for the spatial derivative. Combining the characteristic method and the hybridized discontinuous Galerkin method, the symmetric variational formulation is constructed. The stability of the presented scheme is proved. Theoretically, the order of $\mathcal{O}(h^{k+1/2} + \Delta t)$ is established for the corresponding models and numerically the better convergence rates are detected by carefully choosing the numerical fluxes. Extensive numerical experiments are performed to illustrate the performance of the proposed schemes. The first numerical example is to display the convergence orders, while the second one justifies the benefits of the schemes. Both are tested with triangular meshes.

Keywords 2D fractional convection–diffusion equations · Hybridized discontinuous Galerkin method · Symmetric variational formula · Triangular meshes

Mathematics Subject Classification 26A33 · 35R11 · 65M60 · 65M12

✉ Jinyun Yuan
yuanjy@gmail.com

Shuqin Wang
wsqlzu@gmail.com

Weihua Deng
dengwh@lzu.edu.cn

Yujiang Wu
myjaw@lzu.edu.cn

[1] School of Mathematics and Statistics, Gansu Key Laboratory of Applied Mathematics and Complex Systems, Lanzhou University, Lanzhou 730000, People's Republic of China

[2] Department of Mathematics, Centro Politécnico, Federal University of Paraná, CP: 19.089, Curitiba, PR CEP: 81531-980, Brazil

1 Introduction

Fractional differential equations (FDEs) have become more and more popular in applied science and engineering field recently. The history and mathematical background of fractional differential operators are given in [25] with definitions and applications of fractional calculus. This kind of equations has been used increasingly in many fields, for example, in Nature [16] fractional operators applied in fractal stream chemistry and its implications for contaminant transport in catchments, in [19] the fractional calculus motivated into bioengineering, and its application as a model for physical phenomena exhibiting anomalous diffusion, L*é*vy motion, turbulence [1,2,28], etc.

Let us briefly review the development of numerical methods for the fractional convection–diffusion equations. Several authors have proposed a variety of high-order finite difference schemes for solving time-fractional convection–diffusion equations, for example [10,17,29,31], and solving space-fractional convection–diffusion equations [6,18]. In [20,21,23], W. Mclean and K. Mustapha have used the piecewise-constant and piecewise-linear discontinuous Galerkin (DG) methods to solve the time-fractional diffusion and wave equations, respectively. But these methods require more computational costs. In order to tackle those problems, in [22] W. Mclean has proposed an efficient scheme called fast summation by interval clustering to reduce the implementation memory; more recent works on this issue can been in [9,24]. Furthermore, in [11] Deng and Hesthaven have developed DG methods for fractional spatial derivatives and given a fundamental frame to combine the DG methods with fractional operators. In [30] Xu and Hesthaven have applied the DG methods to the fractional convection–diffusion equations in one dimension. In the two dimensional case, Ji and Tang [15] have applied the DG methods to recast the fractional diffusion equations in rectangular meshes with the numerically optimal convergence order $\mathcal{O}(h^{k+1})$. However, there are no theoretical results. So far very few literatures deal with the fractional problems in triangular meshes, besides [26]. This motives us to consider a successful DG method for solving the fractional problems in triangular meshes.

Here, we consider the time-dependent space-fractional convection–diffusion problem

$$\begin{cases} \partial_t u + \boldsymbol{b}\cdot\nabla u - \frac{\partial^\alpha u}{\partial x^\alpha} - \frac{\partial^\beta u}{\partial y^\beta} = f, & (x,y,t)\in\Omega\times J,\\ u(x,y,0) = u_0(x,y), & (x,y)\in\Omega,\\ u(x,y,t) = 0, & (x,y,t)\in\partial\Omega\times J, \end{cases} \tag{1.1}$$

in the domain $\Omega = (a,b)\times(c,d)$ and $J = [0,T]$ with the superdiffusion operators which are defined by the left Riemann–Liouville fractional derivatives $\frac{\partial^\alpha u}{\partial x^\alpha}$ and $\frac{\partial^\beta u}{\partial y^\beta}$, $1<\alpha,\beta<2$. The function $f\in L^2(J;L^2(\Omega))$ is a source term; the convection coefficient $\boldsymbol{b}$ is supposed to satisfy $\boldsymbol{b}\in L^\infty(J;W^{1,\infty}(\Omega)^2)$, and the initial function $u\in L^2(\Omega)$.

In this work, we shall design a stable and accurate DG method for (1.1). The stability and convergence are proved in multi-dimensional case. This development is built on the extension of the previous DG works found in [11,30], where a qualitative study of the high-order local DG methods was discussed and some theoretical results were offered in one space dimension. In order to perform the error analysis, the authors defined some projection operators to prove the convergence results. Unfortunately, the defined projection operators can not be easily extended to two dimensional case (see [11,30]). Hence, to avoid this difficulty, a different DG method is designed in this paper by carefully choosing the numerical fluxes and adding penalty terms. The presented hybridized discontinuous Galerkin (HDG) method has the following attractive properties: (1) The HDG method can be used for other fractional

problems, for example, fractional diffusion equations; (2) It has excellent provable stability, i.e., the stability can be proved in any space dimensions; (3) Theoretically, the error analysis can be more easily performed with the general analytical methods in any space dimensions.

The outline of this paper is as follows. In Sect. 2, we introduce some basic definitions, notations and review a few lemmas which are useful for the following analysis. In Sect. 3, we present the computational schemes and give some discussions. In Sect. 4, we perform the stability and convergence analysis for the 2D space-fractional convection–diffusion equations. In Sect. 5, we make the numerical experiments and show some simulation results to verify the theoretical results and illustrate the performance of the proposed schemes. We conclude the paper with some remarks in the last section.

2 Preliminaries

In the following we give some definitions of fractional integrals, derivatives, and their properties.

Definition 1 ([25]) For any $\mu > 0$, the left and right Riemann–Liouville fractional integrals of function $u(x)$ defined on (a, b) are defined by

$$ {}_aI_x^{\mu}u(x) = \int_a^x \frac{(x-\xi)^{\mu-1}}{\Gamma(\mu)}u(\xi)d\xi, $$

and

$$ {}_xI_b^{\mu}u(x) = \int_x^b \frac{(\xi-x)^{\mu-1}}{\Gamma(\mu)}u(\xi)d\xi. $$

Definition 2 ([25]) For any $\mu > 0, n-1 < \mu < n, n \in N^+$, the left and right Riemann–Liouville fractional derivatives of function u defined on (a, b) are defined by

$$ {}_aD_x^{\mu}u(x) = \frac{d^n}{dx^n}\int_a^x \frac{(x-\xi)^{n-\mu-1}}{\Gamma(n-\mu)}u(\xi)d\xi, $$

and

$$ {}_xD_b^{\mu}u(x) = (-1)^n\frac{d^n}{dx^n}\int_x^b \frac{(\xi-x)^{n-\mu-1}}{\Gamma(n-\mu)}u(\xi)d\xi. $$

Definition 3 ([25]) For any $\mu > 0, n-1 < \mu < n, n \in N^+$, Caputo's left and right fractional derivatives of function $u(x)$ on (a, b) are defined by

$$ {}_a^CD_x^{\mu}u(x) = \int_a^x \frac{(x-\xi)^{n-\mu-1}}{\Gamma(n-\mu)}\frac{d^nu(\xi)}{d\xi^n}d\xi, $$

and

$$ {}_x^CD_b^{\mu}u(x) = \int_x^b \frac{(\xi-x)^{n-\mu-1}}{\Gamma(n-\mu)}\frac{(-1)^nd^nu(\xi)}{d\xi^n}d\xi. $$

Lemma 1 (Adjoint property [11,13,30]) *For any $\mu > 0$, the left and right Riemann–Liouville fractional integral operators are adjoints for any functions $u(x), v(x) \in L^2(a, b)$, i.e.,*

$$ \int_a^b {}_aI_x^{\mu}u(x)v(x)dx = \int_a^b u(x){}_xI_b^{\mu}v(x)dx. \tag{2.1} $$

Lemma 2 ([11,30]) *Suppose that $u(x)$ is a function defined on (a,b), $u^{(k)}(x)=0$ when $x=a$ or $x=b$, $\forall\, 0\le k\le n-1$ $(n-1<\mu<n)$, $n\in N^+$. There are*

$$ {}_aD_x^{\mu}u(x)=D^n\,{}_aI_x^{n-\mu}u(x)={}_aI_x^{n-\mu}\big(D^nu(x)\big), $$

or

$$ {}_xD_b^{\mu}u(x)=(-D)^n\,{}_xI_b^{n-\mu}u(x)={}_xI_b^{n-\mu}\big((-D)^nu(x)\big). $$

Note that, from Definitions 2, 3 and Lemma 2 if the solution u of (1.1) satisfies $u(x,y)=0$ when $x=a$ or $y=c$, then for any $1<\alpha,\beta<2$, the left fractional Riemann–Liouville derivatives of function $u(x,y)$ on $\Omega=(a,b)\times(c,d)$ can be rewritten as (see [11,30]):

$$ \frac{\partial^{\alpha}u}{\partial x^{\alpha}}=\frac{\partial}{\partial x}\,{}_aI_x^{2-\alpha}\left(\frac{\partial}{\partial x}u(x,y)\right), \tag{2.2} $$

$$ \frac{\partial^{\beta}u}{\partial y^{\beta}}=\frac{-\partial}{\partial y}\,{}_cI_y^{2-\beta}\left(\frac{-\partial}{\partial y}u(x,y)\right). \tag{2.3} $$

For the convenience, we use the notation

$$ I_{\boldsymbol{x}}^{\vec{\boldsymbol{\alpha}}}=\left({}_aI_x^{\alpha_1},\,{}_cI_y^{\alpha_2}\right), \tag{2.4} $$

where $(\alpha_1,\alpha_2)=(2-\alpha,2-\beta)$ and $\alpha_1,\alpha_2\in(0,1)$.

Definition 4 (*The left and right fractional spaces* [11]) For $0<\mu<1$, extend $u(x)$ outside of $\mathfrak{I}:=(a,b)$ by zero. Define the norms

$$ \|u\|_{J_L^{-\mu}(\mathbb{R})}:=\|_{-\infty}I_x^{\mu}u\|_{L^2(\mathbb{R})}, \tag{2.5} $$

$$ \|u\|_{J_R^{-\mu}(\mathbb{R})}:=\|_xI_{\infty}^{\mu}u\|_{L^2(\mathbb{R})}. \tag{2.6} $$

Let the two spaces $J_L^{-\mu}(\mathbb{R})$ and $J_R^{-\mu}(\mathbb{R})$ denote the closures of $C_0^{\infty}(\mathbb{R})$ with respect to $\|\cdot\|_{J_L^{-\mu}}$ and $\|\cdot\|_{J_R^{-\mu}}$, respectively.

Lemma 3 ([11,13,30]) *For $\mu>0$, assume that $u(x)$ is a real function. Then*

$$ \left({}_{-\infty}I_x^{\mu}u,{}_xI_{\infty}^{\mu}u\right)=cos(\mu\pi)\,\|u\|^2_{J_L^{-\mu}(\mathbb{R})}=cos(\mu\pi)\,\|u\|^2_{J_R^{-\mu}(\mathbb{R})}. \tag{2.7} $$

Generally, we consider the case in which the problem is in a bounded domain instead of $\mathbb{R}$. Thus we restrict the definitions to $\mathfrak{I}=(a,b)$.

Definition 5 ([11,30]) Define the spaces $J_{L,0}^{-\mu}(\mathfrak{I})$ and $J_{R,0}^{-\mu}(\mathfrak{I})$ as the closures of $C_0^{\infty}(\mathfrak{I})$ under their respective norms.

Theorem 4 ([11,30]) *If $-\mu_2<-\mu_1<0$, then $J_{L,0}^{-\mu_1}(\mathfrak{I})$ and $J_{R,0}^{-\mu_1}(\mathfrak{I})$ are embedded into $J_{L,0}^{-\mu_2}(\mathfrak{I})$ and $J_{R,0}^{-\mu_2}(\mathfrak{I})$, respectively. Furthermore, $L^2(\mathfrak{I})$ is embedded into both of them.*

Definition 6 ([11,30]) By Lemmas 1, 3, Definitions 4 and 5, we obtain

$$ \int_c^d\left({}_aI_x^{\alpha_1}u(\cdot,y),u(\cdot,y)\right)_{L^2(a,b)}dy=cos(\alpha_1\pi/2)\int_c^d\|u(\cdot,y)\|^2_{J_{R,0}^{-\alpha_1/2}(a,b)}dy, \tag{2.8} $$

$$ \int_a^b\left({}_cI_y^{\alpha_2}u(x,\cdot),u(x,\cdot)\right)_{L^2(c,d)}dx=cos(\alpha_2\pi/2)\int_a^b\|u(x,\cdot)\|^2_{J_{R,0}^{-\alpha_2/2}(c,d)}dx. \tag{2.9} $$

Let the spaces $J_{R,0}^{-\alpha_1/2}(a,b)$ and $J_{R,0}^{-\alpha_2/2}(c,d)$ denote the closures of $C_0^{\infty}(a,b)$ and $C_0^{\infty}(c,d)$ under their respective norms, and $\alpha_1=2-\alpha$, $\alpha_2=2-\beta$, $\alpha_1,\alpha_2\in(0,1)$.

3 Derivation of the Numerical Schemes

We first review some notations, and then focus on deriving the fully discrete numerical scheme of the 2D space-fractional convection–diffusion equation.

3.1 Notations

For the mathematical setting of the DG methods, we describe some spaces and notations. The domain Ω is subdivided into elements E. Here E is a triangle in 2D. We assume that the intersection of two elements is either empty, or an edge (2D). The mesh is called regular if

$$\forall E \in \mathscr{E}_h, \quad \frac{h_E}{\rho_E} \leq C,$$

where $\mathscr{E}_h$ is the subdivision of Ω, C a constant, h_E the diameter of the element E, and ρ_E the diameter of the inscribed circle in element E. Throughout this work $h = \max_{E\in\mathscr{E}_h} h_E$.

We introduce the broken Sobolev space for any real numbers s by

$$H^s(\mathscr{E}_h) = \left\{v \in L^2(\Omega) : \forall E \in \mathscr{E}_h, v|_E \in H^s(E)\right\},$$

equipped with the broken Sobolev norm:

$$\| v \|_{H^s(\mathscr{E}_h)} = \left(\sum_{E\in\mathscr{E}_h} \| v \|^2_{H^s(E)}\right)^{\frac{1}{2}}.$$

The set of edges of the subdivision $\mathscr{E}_h$ is denoted by $\mathscr{E}_h^B$. Let $\mathscr{E}_h^i$ denote the set of interior edges, and $\mathscr{E}_h^b = \mathscr{E}_h^B \setminus \mathscr{E}_h^i$ denote the set of edges on $\partial\Omega$. With each edge e, the unit normal vector is $\boldsymbol{n}_e$. If e is on the boundary $\partial\Omega$, then $\boldsymbol{n}_e$ is taken to be the unit outward vector normal to $\partial\Omega$ [27].

If v belongs to $H^1(\mathscr{E}_h)$, then the trace of v along any side of one element E is well defined. If two elements E_1^e and E_2^e are neighbours and share one common side e, then there are two traces of v belonging to e. We assume that the normal vector $\boldsymbol{n}_e$ is oriented from E_1^e to E_2^e. Then the average and jump are defined, respectively, by

$$\{v\} = \frac{1}{2}(v|_{\partial E_1^e} + v|_{\partial E_2^e}), \quad [\![v]\!] = (v|_{\partial E_1^e} - v|_{\partial E_2^e}), \ \forall e \in \partial E_1^e \bigcap \partial E_2^e.$$

If e is on $\partial\Omega$, we have

$$\{v\} = [\![v]\!] = v|_e, \quad \forall e \in \partial E \bigcap \partial\Omega.$$

3.2 HDG Scheme

For designing the DG method of fractional derivative, we rewrite (1.1) as a low order system (see [11,30]). Firstly, we introduce two auxiliary variables $\boldsymbol{p}, \boldsymbol{\sigma}$ and set

$$\begin{cases} \boldsymbol{p} = \nabla u, \\ \boldsymbol{\sigma} = I_{\boldsymbol{x}}^{\bar{\boldsymbol{\alpha}}} \boldsymbol{p} = \left({}_aI_x^{\alpha_1} p_x, {}_cI_y^{\alpha_2} p_y\right). \end{cases}$$

As Ref. [4], let $\psi(\boldsymbol{x}, t) = (1 + |\boldsymbol{b}(\boldsymbol{x}, t)|^2)^{\frac{1}{2}}$, where $|\boldsymbol{b}(\boldsymbol{x}, t)|^2 = b_1^2 + b_2^2$. Hence, the characteristic direction associated with $\partial_t u + \boldsymbol{b}\cdot\nabla u$ is denoted by $\partial_\tau = \frac{\partial_t}{\psi} + \frac{\boldsymbol{b}\cdot\nabla}{\psi}$. Then, from (2.2) and (2.3), Eq. (1.1) can be rewritten as a mixed form [3,7,8,11,30]:

$$\begin{cases} \psi \partial_\tau u - \nabla \cdot \boldsymbol{\sigma} = f, & (x, y, t) \in \Omega \times J, \\ \boldsymbol{\sigma} - I_{\boldsymbol{x}}^{\tilde{\boldsymbol{\alpha}}} \boldsymbol{p} = 0, & (x, y, t) \in \Omega \times J, \\ \boldsymbol{p} - \nabla u = 0, & (x, y, t) \in \Omega \times J, \\ u(x, y, 0) = u_0(x, y), & (x, y) \in \Omega, \\ u(x, y, t) = 0, & (x, y, t) \in \partial\Omega \times J, \end{cases} \tag{3.1}$$

where $I_{\boldsymbol{x}}^{\tilde{\boldsymbol{\alpha}}}$ is defined in (2.4).

For an arbitrary subset $E \in \mathscr{E}_h$, we multiply the first, second, and the third equation of (3.1) by the smooth test functions v, $\boldsymbol{\omega}$, and $\boldsymbol{q}$, respectively. In order to obtain a symmetric weak variational formulation, we only integrate the first equation of (3.1) by parts, and obtain

$$\begin{cases} \int_E \psi \partial_\tau u v d\boldsymbol{x} + \int_E \boldsymbol{\sigma} \cdot \nabla v d\boldsymbol{x} - \int_{\partial E} \boldsymbol{\sigma} \cdot \boldsymbol{n}_E v ds = \int_E f v d\boldsymbol{x}, \\ \int_E \boldsymbol{\sigma} \cdot \boldsymbol{\omega} d\boldsymbol{x} - \int_E I_{\boldsymbol{x}}^{\tilde{\boldsymbol{\alpha}}} \boldsymbol{p} \cdot \boldsymbol{\omega} d\boldsymbol{x} = 0, \\ \int_E \boldsymbol{p} \cdot \boldsymbol{q} d\boldsymbol{x} - \int_E \nabla u \cdot \boldsymbol{q} d\boldsymbol{x} = 0, \end{cases} \tag{3.2}$$

where $\boldsymbol{n}_E$ is the outward unit normal to ∂E. Note that the above equations are well defined for the functions $(u, \boldsymbol{\sigma}, \boldsymbol{p})$ and $(v, \boldsymbol{\omega}, \boldsymbol{q})$ in $\mathbb{V} \times \mathbb{Q} \times \mathbb{Q}$, where

$$\mathbb{V} = \left\{ u \in L^2(\Omega) : u|_E \in H^1(E), \ \forall E \in \mathscr{E}_h \right\},$$
$$\mathbb{Q} = \left\{ \boldsymbol{p} \in (L^2(\Omega))^2 : \boldsymbol{p}|_E \in (H^1(E))^2, \quad \forall E \in \mathscr{E}_h \right\}.$$

Next we will approximate the exact solution $(u, \boldsymbol{\sigma}, \boldsymbol{p})$ with the functions $(u_h, \boldsymbol{\sigma}_h, \boldsymbol{p}_h)$ in the finite element spaces $\mathbb{V}_h \times \mathbb{Q}_h \times \mathbb{Q}_h \subset \mathbb{V} \times \mathbb{Q} \times \mathbb{Q}$, where

$$\mathbb{V}_h = \left\{ u_h \in L^2(\Omega) : u_h|_E \in P^k(E), \ \forall E \in \mathscr{E}_h \right\},$$
$$\mathbb{Q}_h = \left\{ \boldsymbol{p}_h \in (L^2(\Omega))^2 : \boldsymbol{p}_h|_E \in (P^k(E))^2, \ \forall E \in \mathscr{E}_h \right\},$$

where the finite element space $P^k(E)$ denotes the set of polynomials of degree less than or equal to $k \geq 0$.

Thus, the approximate solution $(u_h, \boldsymbol{\sigma}_h, \boldsymbol{p}_h)$ satisfies the weak formulation, for all $(v, \boldsymbol{\omega}, \boldsymbol{q}) \in \mathbb{V}_h \times \mathbb{Q}_h \times \mathbb{Q}_h$,

$$\begin{cases} \int_E \psi \partial_\tau u_h v d\boldsymbol{x} + \int_E \boldsymbol{\sigma}_h \cdot \nabla v d\boldsymbol{x} - \int_{\partial E} \boldsymbol{\sigma}_h^\star \cdot \boldsymbol{n}_E v ds = \int_E f v d\boldsymbol{x}, \\ \int_E \boldsymbol{\sigma}_h \cdot \boldsymbol{\omega} d\boldsymbol{x} - \int_E I_{\boldsymbol{x}}^{\tilde{\boldsymbol{\alpha}}} \boldsymbol{p}_h \cdot \boldsymbol{\omega} d\boldsymbol{x} = 0, \\ \int_E \boldsymbol{p}_h \cdot \boldsymbol{q} d\boldsymbol{x} - \int_E \nabla u_h \cdot \boldsymbol{q} d\boldsymbol{x} = 0, \end{cases} \tag{3.3}$$

where the numerical fluxes are well chosen as $\boldsymbol{\sigma}_h^\star = \{\boldsymbol{\sigma}_h\}$, $\forall e \in \mathscr{E}_h^B$ in order to ensure the stability of the scheme and its accuracy.

It is well known that the fluxes $\boldsymbol{\sigma}_h^\star = \{\boldsymbol{\sigma}_h\}$ are consistent. Inspired by the penalty Galerkin methods [27] and noting the fact that $[\![u]\!]\big|_e = 0, \forall e \in \mathscr{E}_h^B$ and $[\![\boldsymbol{\sigma}]\!] = 0, \forall e \in \mathscr{E}_h^i$, a symmetric and stable DG scheme is derived as follows. Substituting the flux $\boldsymbol{\sigma}_h^\star = \{\boldsymbol{\sigma}_h\}$ into (3.3), summing over all the elements, and adding the penalty terms, we observe that for $(u_h, \boldsymbol{\sigma}_h, \boldsymbol{p}_h) \in \mathbb{V}_h \times \mathbb{Q}_h \times \mathbb{Q}_h$, the semi-discrete variational formulation is given by

$$\begin{cases} (\psi \partial_\tau u_h, v) + (\boldsymbol{\sigma}_h, \nabla v) - (\{\boldsymbol{\sigma}_h\} \cdot \boldsymbol{n}_e, [\![v]\!])_{\mathscr{E}_h^B} + \varepsilon_1([\![u_h]\!], [\![v]\!])_{\mathscr{E}_h^B} = (f, v), \\ (\boldsymbol{\sigma}_h, \boldsymbol{\omega}) - \left(I_{\boldsymbol{x}}^{\tilde{\boldsymbol{\alpha}}} \boldsymbol{p}_h, \boldsymbol{\omega}\right) = 0, \\ (\boldsymbol{p}_h, \boldsymbol{q}) - (\nabla u_h, \boldsymbol{q}) + ([\![u_h]\!], \{\boldsymbol{q}\} \cdot \boldsymbol{n}_e)_{\mathscr{E}_h^B} + \varepsilon_2([\![\boldsymbol{\sigma}_h]\!], [\![\boldsymbol{q}]\!])_{\mathscr{E}_h^i} = 0. \end{cases} \tag{3.4}$$

For any $(v, \boldsymbol{\omega}, \boldsymbol{q}) \in \mathbb{V}_h \times \mathbb{Q}_h \times \mathbb{Q}_h$, the exact solution of (1.1) is expected to be continuously differentiable with respect to the variables x and y, which keeps the consistency of the scheme. The term $(\llbracket u \rrbracket, \{\boldsymbol{q}\} \cdot \boldsymbol{n}_e)_{\mathscr{E}_h^B}$ vanishes since the exact solution u satisfies $\llbracket u \rrbracket\big|_e = 0, \forall e \in \mathscr{E}_h^B$. Note that $\varepsilon_1(\llbracket u \rrbracket, \llbracket v \rrbracket)_{\mathscr{E}_h^B}$ penalizes the jump of the function u, whereas $\varepsilon_2(\llbracket \boldsymbol{\sigma} \rrbracket, \llbracket \boldsymbol{q} \rrbracket)_{\mathscr{E}_h^i}$ penalizes the jump of the function $\boldsymbol{\sigma}$. Here ε_1 and ε_2 are the positive constants to be chosen. Unfortunately the third equation of (3.4) makes the DG method lose its locality, since $\boldsymbol{p}_h$ is a function of u_h and $\boldsymbol{\sigma}_h$, $\boldsymbol{p}_h$ can not be eliminated from the third equation. So we have to simultaneously solve the three unknowns u_h, p_{xh}, p_{yh}. Although the extra unknowns can not be eliminated in the HDG methods, our choice of fluxes makes the error analysis available. Above and throughout, the following notations are used,

$$(w, v) = \sum_{E \in \mathscr{E}_h} (w, v)_E, \ (w, v)_{\mathscr{E}_h^i} = \sum_{e \in \mathscr{E}_h^i} (w, v)_e, \ (w, v)_{\mathscr{E}_h^B} = \sum_{e \in \mathscr{E}_h^B} (w, v)_e.$$

3.3 Dealing with Time

After performing the HDG approximation, we discretize the time derivative with the characteristic method. For the given positive integer N, let $0 = t^0 < t^1 < \cdots < t^N = T$ be a partition of J into subintervals $J^n = (t^{n-1}, t^n]$ with uniform mesh and the interval length $\Delta t = t^n - t^{n-1}, 1 \le n \le N$. The characteristic tracing back along the field $\boldsymbol{b}$ of a point $\boldsymbol{x} = (x, y) \in \Omega$ at time t^n to t^{n-1} is approximated by [4,5,12]

$$\check{\boldsymbol{x}}(\boldsymbol{x}, t^{n-1}) = \boldsymbol{x} - \boldsymbol{b}(\boldsymbol{x}, t^n)\Delta t.$$

Therefore, the approximation for the hyperbolic part of (1.1) at time t^n can be approximated as

$$\psi^n \partial_\tau u^n \approx \frac{u^n - \check{u}^{n-1}}{\Delta t},$$

where $u^n = u(\boldsymbol{x}, t^n)$, $\check{u}^{n-1} = u(\check{\boldsymbol{x}}(\boldsymbol{x}, t^{n-1}), t^{n-1})$, and $\check{u}^0 = u^0(\boldsymbol{x})$.

Remark 1 (see [12]) Assume that the solution u of (1.1) is sufficiently regular. Under the assumption of the function $\boldsymbol{b}$, we have

$$\left\| \psi^n \partial_\tau u^n - \frac{u^n - \check{u}^{n-1}}{\Delta t} \right\|_{L^2(\Omega)}^2 \le C \parallel \psi^{(4)} \parallel_{L^\infty(J;L^\infty(\Omega))} \parallel \partial_{\tau\tau} u \parallel_{L^2(J^n;L^2(\Omega))}^2 \Delta t.$$

Thus, the fully discrete scheme corresponding to the variational formulation (3.4) is to find $(u_h^n, \boldsymbol{\sigma}_h^n, \boldsymbol{p}_h^n) \in \mathbb{V}_h \times \mathbb{Q}_h \times \mathbb{Q}_h$, for any $(v, \boldsymbol{\omega}, \boldsymbol{q}) \in \mathbb{V}_h \times \mathbb{Q}_h \times \mathbb{Q}_h$, such that

$$\begin{cases} \left(\frac{u_h^n - \check{u}_h^{n-1}}{\Delta t}, v \right) + \left(\boldsymbol{\sigma}_h^n, \nabla v \right) - (\{\boldsymbol{\sigma}_h^n\} \cdot \boldsymbol{n}_e, \llbracket v \rrbracket)_{\mathscr{E}_h^B} + \varepsilon_1(\llbracket u_h^n \rrbracket, \llbracket v \rrbracket)_{\mathscr{E}_h^B} = (f^n, v), \\ \left(\boldsymbol{\sigma}_h^n, \boldsymbol{\omega} \right) - \left(I_{\boldsymbol{x}}^{\tilde{\alpha}} \boldsymbol{p}_h^n, \boldsymbol{\omega} \right) = 0, \\ \left(\boldsymbol{p}_h^n, \boldsymbol{q} \right) - \left(\nabla u_h^n, \boldsymbol{q} \right) + (\llbracket u_h^n \rrbracket, \{\boldsymbol{q}\} \cdot \boldsymbol{n}_e)_{\mathscr{E}_h^B} + \varepsilon_2(\llbracket \boldsymbol{\sigma}_h^n \rrbracket, \llbracket \boldsymbol{q} \rrbracket)_{\mathscr{E}_h^i} = 0, \end{cases} \tag{3.5}$$

where $\check{u}_h^{n-1} = u_h(\check{\boldsymbol{x}}(\boldsymbol{x}, t^{n-1}), t^{n-1})$, $\check{u}_h^0 = u^0$.

Define the bilinear forms by

$$\mathfrak{a}\left(\boldsymbol{\sigma}_h^n, v\right) := \left(\boldsymbol{\sigma}_h^n, \nabla v\right) - \left(\left\{\boldsymbol{\sigma}_h^n\right\} \cdot \boldsymbol{n}_e, \llbracket v \rrbracket\right)_{\mathscr{E}_h^B}, \quad \mathfrak{c}\left(\boldsymbol{p}_h^n, \boldsymbol{q}\right) := \left(\boldsymbol{p}_h^n, \boldsymbol{q}\right),$$
$$\mathfrak{d}\left(u_h^n, v\right) := \varepsilon_1(\llbracket u_h^n \rrbracket, \llbracket v \rrbracket)_{\mathscr{E}_h^B}, \quad \mathfrak{e}(\boldsymbol{\sigma}_h^n, \boldsymbol{q}) := \varepsilon_2\left(\llbracket \boldsymbol{\sigma}_h^n \rrbracket, \llbracket \boldsymbol{q} \rrbracket\right)_{\mathscr{E}_h^i},$$

and the linear form

$$\mathscr{F}(v) := (f^n, v) \quad \forall v \in \mathbb{V}_h.$$

We can rewrite (3.5) as a compact formulation: Find $(u_h^n, \boldsymbol{\sigma}_h^n, \boldsymbol{p}_h^n) \in \mathbb{V}_h \times \mathbb{Q}_h \times \mathbb{Q}_h$ at time $t = t^n$, such that

$$\begin{cases} \left(\frac{u_h^n - \check{u}_h^{n-1}}{\Delta t}, v\right) + \mathbb{a}(\boldsymbol{\sigma}_h^n, v) + \mathbb{d}(u_h^n, v) = \mathscr{F}(v), & \forall v \in \mathbb{V}_h, \\ \mathbb{c}(\boldsymbol{\sigma}_h^n, \boldsymbol{\omega}) - \mathbb{c}(I_{\boldsymbol{x}}^{\tilde{\boldsymbol{\alpha}}} \boldsymbol{p}_h^n, \boldsymbol{\omega}) = 0, & \forall \boldsymbol{\omega} \in \mathbb{Q}_h, \\ \mathbb{c}(\boldsymbol{p}_h^n, \boldsymbol{q}) - \mathbb{a}(\boldsymbol{q}, u_h^n) + \mathbb{e}(\boldsymbol{\sigma}_h^n, \boldsymbol{q}) = 0, & \forall \boldsymbol{q} \in \mathbb{Q}_h. \end{cases} \tag{3.6}$$

4 Stability Analysis and Error Estimate

This section focuses on providing the proof of the unconditional stability and the error estimates of the schemes.

4.1 Stability Analysis

In the following, C indicates a generic constant independent of h and Δt, which takes different values in different occurrences.

Lemma 5 ([4]) *If $\boldsymbol{b} \in L^\infty(J; W^{1,\infty}(\Omega)^2)$, for any function $v \in L^2(\Omega)$ and each n, there is*

$$\| \check{v} \|_{L^2(\Omega)}^2 - \| v \|_{L^2(\Omega)}^2 \leq C \Delta t \| v \|_{L^2(\Omega)}^2, \tag{4.1}$$

where $\check{v}(\boldsymbol{x}) = v(\boldsymbol{x} - \boldsymbol{b}(\boldsymbol{x}, t^n)\Delta t)$.

Theorem 6 (Numerical stability) *If $\boldsymbol{b} \in L^\infty(J; W^{1,\infty}(\Omega)^2)$, the HDG scheme (3.5) is stable, i.e., for any integer $N = 1, 2, \ldots$, there is*

$$\| u_h^N \|_{L^2(\Omega)}^2 + 2\Delta t \sum_{n=1}^{N} \left|(u_h^n, \boldsymbol{\sigma}_h^n, \boldsymbol{p}_h^n)\right|_{\mathscr{A}}^2 \leq C \Delta t \sum_{n=1}^{N} \| f^n \|_{L^2(\Omega)}^2 + C \| u^0 \|_{L^2(\Omega)}^2, \tag{4.2}$$

where $u_h^0 = u^0$, and the semi-norm $|\cdot|_{\mathscr{A}}$ is defined as

$$\begin{aligned} &\left|(u_h^n, \boldsymbol{\sigma}_h^n, \boldsymbol{p}_h^n)\right|_{\mathscr{A}}^2 \\ &= \mathbb{d}(u_h^n, u_h^n) + \mathbb{c}(I_{\boldsymbol{x}}^{\tilde{\boldsymbol{\alpha}}} \boldsymbol{p}_h^n, \boldsymbol{p}_h^n) + \mathbb{e}(\boldsymbol{\sigma}_h^n, \boldsymbol{\sigma}_h^n) \\ &= \cos(\alpha_1 \pi/2) \int_c^d \| p_{xh}^n(\cdot, y) \|_{J_{R,0}^{-\alpha_1/2}(a,b)}^2 \, dy + \varepsilon_1 \sum_{e \in \mathscr{E}_h^B} \| [\![u_h^n]\!] \|_{L^2(e)}^2 \\ &\quad + \cos(\alpha_2 \pi/2) \int_a^b \| p_{yh}^n(x, \cdot) \|_{J_{R,0}^{-\alpha_2/2}(c,d)}^2 \, dx + \varepsilon_2 \sum_{e \in \mathscr{E}_h^i} \| [\![\boldsymbol{\sigma}_h^n]\!] \|_{L^2(e)}^2 . \end{aligned} \tag{4.3}$$

Proof Let $v = 2\Delta t u_h^n$, $\boldsymbol{\omega} = -2\Delta t \boldsymbol{p}_h^n$, $\boldsymbol{q} = 2\Delta t \boldsymbol{\sigma}_h^n$ in the equations of (3.6), respectively. By the symmetry of the bilinear formulas, adding the above equations, we obtain

$$2\Delta t \mathscr{F}(u_h^n) = 2\Delta t \mathbb{c}(I_{\boldsymbol{x}}^{\tilde{\boldsymbol{\alpha}}} \boldsymbol{p}_h^n, \boldsymbol{p}_h^n) + 2\Delta t \mathbb{e}(\boldsymbol{\sigma}_h^n, \boldsymbol{\sigma}_h^n) + 2\left(u_h^n - \check{u}_h^{n-1}, u_h^n\right) + 2\Delta t \mathbb{d}(u_h^n, u_h^n).$$

Following from

$$2\left(u_h^n-\check{u}_h^{n-1},u_h^n\right)\geq\|\,u_h^n\,\|_{L^2(\Omega)}^2-\|\,\check{u}_h^{n-1}\,\|_{L^2(\Omega)}^2,$$

the Young inequality, the definition of $\mathscr{F}$ and $|\cdot|_{\mathscr{A}}$, and Lemma 5, we have

$$\begin{aligned}&\|\,u_h^n\,\|_{L^2(\Omega)}^2-\|\,u_h^{n-1}\,\|_{L^2(\Omega)}^2+2\Delta t\left|(u_h^n,\boldsymbol{\sigma}_h^n,\boldsymbol{p}_h^n)\right|_{\mathscr{A}}^2\\&\quad\leq C\Delta t\,\|\,u_h^{n-1}\,\|_{L^2(\Omega)}^2+\Delta t\left(\|\,u_h^n\,\|_{L^2(\Omega)}^2+\|\,f^n\,\|_{L^2(\Omega)}^2\right).\end{aligned}$$

Summing from $n=1,2,\ldots,N$, we get

$$\begin{aligned}&\|\,u_h^N\,\|_{L^2(\Omega)}^2+2\Delta t\sum_{n=1}^{N}\left|(u_h^n,\boldsymbol{\sigma}_h^n,\boldsymbol{p}_h^n)\right|_{\mathscr{A}}^2\\&\quad\leq C\Delta t\sum_{n=1}^{N}\|\,u_h^n\,\|_{L^2(\Omega)}^2+(1+C\Delta t)\,\|\,u_h^0\,\|_{L^2(\Omega)}^2+\Delta t\sum_{n=1}^{N}\|\,f^n\,\|_{L^2(\Omega)}^2.\end{aligned}$$

Using the discrete Grönwall inequality, with $C\Delta t<1,\ \forall N\geq 1$, there is

$$\|\,u_h^N\,\|_{L^2(\Omega)}^2+2\Delta t\sum_{n=1}^{N}\left|(u_h^n,\boldsymbol{\sigma}_h^n,\boldsymbol{p}_h^n)\right|_{\mathscr{A}}^2\leq C\,\|\,u_h^0\,\|_{L^2(\Omega)}^2+C\Delta t\sum_{n=1}^{N}\|\,f^n\,\|_{L^2(\Omega)}^2.\tag{4.4}$$

4.2 Error Estimates

In this subsection we state and discuss the error bounds for the HDG scheme. The main steps of our error analysis follow the classical methods in finite element analysis, i.e., the so-called Galerkin orthogonality property. As usual, we denote the errors $(e_u^n,\boldsymbol{e}_{\boldsymbol{\sigma}}^n,\boldsymbol{e}_{\boldsymbol{p}}^n)=(u^n-u_h^n,\boldsymbol{\sigma}^n-\boldsymbol{\sigma}_h^n,\boldsymbol{p}^n-\boldsymbol{p}_h^n)$ by

$$\left(e_u^n,\boldsymbol{e}_{\boldsymbol{\sigma}}^n,\boldsymbol{e}_{\boldsymbol{p}}^n\right)=(u^n-\Pi u^n,\boldsymbol{\sigma}^n-\boldsymbol{\Pi}\boldsymbol{\sigma}^n,\boldsymbol{p}^n-\boldsymbol{\Pi}\boldsymbol{p}^n)+\left(\Pi e_u^n,\boldsymbol{\Pi}\boldsymbol{e}_{\boldsymbol{\sigma}}^n,\boldsymbol{\Pi}\boldsymbol{e}_{\boldsymbol{p}}^n\right),$$

where Π and $\boldsymbol{\Pi}=(\Pi,\Pi)$ are the L^2-projection and $(L^2)^2$-projection operators from $\mathbb{V}$ and $\mathbb{Q}$ onto the finite element spaces $\mathbb{V}_h$ and $\mathbb{Q}_h$, respectively. From (3.6), we obtain the compact form

$$\left(\frac{u_h^n-\check{u}_h^{n-1}}{\Delta t},v\right)+\mathscr{A}\left(u_h^n,\boldsymbol{\sigma}_h^n,\boldsymbol{p}_h^n;v,\boldsymbol{\omega},\boldsymbol{q}\right)=\mathscr{F}(v),\tag{4.5}$$

where

$$\begin{aligned}&\mathscr{A}\left(u_h^n,\boldsymbol{\sigma}_h^n,\boldsymbol{p}_h^n;v,\boldsymbol{\omega},\boldsymbol{q}\right)\\&\quad=\mathfrak{a}\left(\boldsymbol{\sigma}_h^n,v\right)+\mathfrak{d}\left(u_h^n,v\right)+\mathfrak{c}\left(\boldsymbol{\sigma}_h^n,\boldsymbol{\omega}\right)-\mathfrak{c}\left(I_{\boldsymbol{x}}^{\bar{\boldsymbol{\alpha}}}\boldsymbol{p}_h^n,\boldsymbol{\omega}\right)+\mathfrak{c}\left(\boldsymbol{p}_h^n,\boldsymbol{q}\right)-\mathfrak{a}\left(\boldsymbol{q},u_h^n\right)+\mathfrak{e}\left(\boldsymbol{\sigma}_h^n,\boldsymbol{q}\right).\end{aligned}\tag{4.6}$$

Lemma 7 *Assume that the solution u of problem (1.1) is sufficiently regular. Then*

$$\begin{aligned}&\left(\psi^n\partial_\tau u^n-\frac{u_h^n-\check{u}_h^{n-1}}{\Delta t},\Pi e_u^n\right)+\left|(\Pi e_u^n,\boldsymbol{\Pi}\boldsymbol{e}_{\boldsymbol{\sigma}}^n,\boldsymbol{\Pi}\boldsymbol{e}_{\boldsymbol{p}}^n)\right|_{\mathscr{A}}^2\\&\quad=\mathscr{A}\left(\Pi u^n-u^n,\boldsymbol{\Pi}\boldsymbol{\sigma}^n-\boldsymbol{\sigma}^n,\boldsymbol{\Pi}\boldsymbol{p}^n-\boldsymbol{p}^n;\Pi e_u^n,-\boldsymbol{\Pi}\boldsymbol{e}_{\boldsymbol{p}}^n,\boldsymbol{\Pi}\boldsymbol{e}_{\boldsymbol{\sigma}}^n\right).\end{aligned}\tag{4.7}$$

Proof By the consistency of the numerical fluxes, the exact solution $(u, \boldsymbol{\sigma}, \boldsymbol{p})$ satisfies (3.4). Taking $v = \Pi e_u^n$, $\boldsymbol{\omega} = -\boldsymbol{\Pi} \boldsymbol{e}_{\boldsymbol{p}}^n$, $\boldsymbol{q} = \boldsymbol{\Pi} \boldsymbol{e}_{\boldsymbol{\sigma}}^n$ and subtracting (3.5) from (3.4) yield

$$\left(\psi^n \partial_\tau u^n - \frac{u_h^n - \check{u}_h^{n-1}}{\Delta t}, \Pi e_u^n\right) + \mathscr{A}\left(e_u^n, \boldsymbol{e}_{\boldsymbol{\sigma}}^n, \boldsymbol{e}_{\boldsymbol{p}}^n; \Pi e_u^n, -\boldsymbol{\Pi} \boldsymbol{e}_{\boldsymbol{p}}^n, \boldsymbol{\Pi} \boldsymbol{e}_{\boldsymbol{\sigma}}^n\right) = 0 \tag{4.8}$$

and

$$\left|(\Pi e_u^n, \boldsymbol{\Pi} \boldsymbol{e}_{\boldsymbol{\sigma}}^n, \boldsymbol{\Pi} \boldsymbol{e}_{\boldsymbol{p}}^n)\right|_{\mathscr{A}}^2 = \mathscr{A}\left(\Pi e_u^n, \boldsymbol{\Pi} \boldsymbol{e}_{\boldsymbol{\sigma}}^n, \boldsymbol{\Pi} \boldsymbol{e}_{\boldsymbol{p}}^n; \Pi e_u^n, -\boldsymbol{\Pi} \boldsymbol{e}_{\boldsymbol{p}}^n, \boldsymbol{\Pi} \boldsymbol{e}_{\boldsymbol{\sigma}}^n\right). \tag{4.9}$$

By the Galerkin orthogonality, there is

$$\begin{aligned} &\mathscr{A}\left(e_u^n, \boldsymbol{e}_{\boldsymbol{\sigma}}^n, \boldsymbol{e}_{\boldsymbol{p}}^n; \Pi e_u^n, -\boldsymbol{\Pi} \boldsymbol{e}_{\boldsymbol{p}}^n, \boldsymbol{\Pi} \boldsymbol{e}_{\boldsymbol{\sigma}}^n\right) \\ &\quad = \mathscr{A}\left(\Pi e_u^n, \boldsymbol{\Pi} \boldsymbol{e}_{\boldsymbol{\sigma}}^n, \boldsymbol{\Pi} \boldsymbol{e}_{\boldsymbol{p}}^n; \Pi e_u^n, -\boldsymbol{\Pi} \boldsymbol{e}_{\boldsymbol{p}}^n, \boldsymbol{\Pi} \boldsymbol{e}_{\boldsymbol{\sigma}}^n\right) \\ &\qquad - \mathscr{A}\left(\Pi u^n - u^n, \boldsymbol{\Pi} \boldsymbol{\sigma}^n - \boldsymbol{\sigma}^n, \boldsymbol{\Pi} \boldsymbol{p}^n - \boldsymbol{p}^n; \Pi e_u^n, -\boldsymbol{\Pi} \boldsymbol{e}_{\boldsymbol{p}}^n, \boldsymbol{\Pi} \boldsymbol{e}_{\boldsymbol{\sigma}}^n\right). \end{aligned} \tag{4.10}$$

Substituting the equalities (4.9) and (4.10) into (4.8) leads to the desired result.

Next we review two lemmas for our analysis. The first one is the standard approximation result for the L^2-projection operator Π from $H^{s+1}(E)$ onto $V_h(E) = \{v; v\big|_E \in P^k(E)\}$ satisfying $\Pi v = v$ for any $v \in P^k(E)$. The second one is the standard trace inequality.

Lemma 8 ([3]) *Let $v \in H^{s+1}(E)$, $s \geq 0$. Π is the L^2-projection operator from $H^{s+1}(E)$ onto $V_h(E)$ such that $\Pi v = v$ for any $v \in P^k(E)$. Then, for $m = 0, 1$,*

$$\begin{cases} \left|v - \Pi v\right|_{H^m(E)} \leq C h_E^{min\{s,k\}+1-m} \parallel v \parallel_{H^{s+1}(E)}, \\ \parallel v - \Pi v \parallel_{L^2(\partial E)} \leq C h_E^{min\{s,k\}+\frac{1}{2}} \parallel v \parallel_{H^{s+1}(E)}. \end{cases} \tag{4.11}$$

Lemma 9 ([3]) *There exists a generic constant C being independent of h_E, for any $v \in V_h(E)$, such that*

$$\parallel v \parallel_{L^2(\partial E)} \leq C h_E^{-\frac{1}{2}} \parallel v \parallel_{L^2(E)}. \tag{4.12}$$

Now we are ready to prove our main results.

4.2.1 The Characteristic Term

In this subsection, we estimate the first left-side term of (4.7).

Lemma 10 ([4]) *If $\boldsymbol{b} \in L^\infty(J; W^{1,\infty}(\Omega)^2)$, for any function $v \in H^1(\Omega)$ and each n,*

$$\parallel v - \check{v} \parallel_{L^2(\Omega)} \leq C \Delta t \parallel \nabla v \parallel_{L^2(\Omega)}, \tag{4.13}$$

where $\check{v} = v(\check{\boldsymbol{x}}) = v(\boldsymbol{x} - \boldsymbol{b}^n \Delta t)$.

The following result is a straightforward consequence of the estimate of the first left-side term of (4.7).

Theorem 11 *Assume that the solution u of problem (1.1) is sufficiently smooth and u_h^n satisfies (3.5). If $\boldsymbol{b} \in L^\infty(J; W^{1,\infty}(\Omega)^2)$, we have*

$$\begin{aligned}
&\left(\psi^n \partial_\tau u^n - \frac{u_h^n - \check{u}_h^{n-1}}{\Delta t}, \Pi e_u^n\right) \\
&\geq \frac{1}{2\Delta t}\left(\| \Pi e_u^n \|_{L^2(\Omega)}^2 - \| \Pi e_u^{n-1} \|_{L^2(\Omega)}^2\right) - C \| \Pi e_u^{n-1} \|_{L^2(\Omega)}^2 \\
&\quad - C\Delta t \| \partial_{\tau\tau} u \|_{L^2(J^n; L^2(\Omega))}^2 - \frac{C}{\Delta t} \| \partial_t (\Pi u - u) \|_{L^2(J^n; L^2(\Omega))}^2 \\
&\quad - C \| \nabla(\Pi u^{n-1} - u^{n-1}) \|_{L^2(\Omega)}^2 - C \| \Pi e_u^n \|_{L^2(\Omega)}^2 .
\end{aligned} \tag{4.14}$$

Proof From (4.7), it can be noted that

$$\begin{aligned}
&\left(\psi^n \partial_\tau u^n - \frac{u_h^n - \check{u}_h^{n-1}}{\Delta t}, \Pi e_u^n\right) \\
&= \left(\frac{\Pi e_u^n - \Pi \check{e}_u^{n-1}}{\Delta t}, \Pi e_u^n\right) + \left(\psi^n \partial_\tau u^n - \frac{u^n - \check{u}^{n-1}}{\Delta t}, \Pi e_u^n\right) \\
&\quad - \left(\frac{(\Pi u^n - u^n) - (\Pi \check{u}^{n-1} - \check{u}^{n-1})}{\Delta t}, \Pi e_u^n\right) \\
&= \sum_{i=1}^{3} \mathscr{B}_i .
\end{aligned} \tag{4.15}$$

Using Lemma 5, we obtain

$$\begin{aligned}
\mathscr{B}_1 &= \left(\frac{\Pi e_u^n - \Pi \check{e}_u^{n-1}}{\Delta t}, \Pi e_u^n\right) \\
&= \frac{1}{2\Delta t}\left(\| \Pi e_u^n \|_{L^2(\Omega)}^2 - \| \Pi \check{e}_u^{n-1} \|_{L^2(\Omega)}^2 + \| \Pi e_u^n - \Pi \check{e}_u^{n-1} \|_{L^2(\Omega)}^2\right) \\
&\geq \frac{1}{2\Delta t}\left(\| \Pi e_u^n \|_{L^2(\Omega)}^2 - \| \Pi \check{e}_u^{n-1} \|_{L^2(\Omega)}^2\right) \\
&\geq \frac{1}{2\Delta t}\left(\| \Pi e_u^n \|_{L^2(\Omega)}^2 - \| \Pi e_u^{n-1} \|_{L^2(\Omega)}^2\right) - C \| \Pi e_u^{n-1} \|_{L^2(\Omega)}^2,
\end{aligned}$$

where $\Pi \check{e}_u^{n-1} = \Pi \check{u}^{n-1} - \check{u}_h^{n-1}$. Also by the Taylor expansion and the Hölder inequality, there are

$$\begin{aligned}
|\, \mathscr{B}_2 \,| &= \left|\left(\psi^n \partial_\tau u^n - \frac{u^n - \check{u}^{n-1}}{\Delta t}, \Pi e_u^n\right)\right| \\
&\leq C\Delta t \| \partial_{\tau\tau} u \|_{L^2(J^n; L^2(\Omega))}^2 + C \| \Pi e_u^n \|_{L^2(\Omega)}^2
\end{aligned}$$

and

$$\begin{aligned}
-\mathscr{B}_3 &= \left(\frac{(\Pi u^n - u^n) - (\Pi \check{u}^{n-1} - \check{u}^{n-1})}{\Delta t}, \Pi e_u^n\right) \\
&= \left(\frac{(\Pi u^n - u^n) - (\Pi u^{n-1} - u^{n-1})}{\Delta t}, \Pi e_u^n\right) \\
&\quad + \left(\frac{(\Pi u^{n-1} - u^{n-1}) - (\Pi \check{u}^{n-1} - \check{u}^{n-1})}{\Delta t}, \Pi e_u^n\right)
\end{aligned}$$

$$= \mathscr{S}_1 + \mathscr{S}_2,$$

where

$$\begin{aligned}\mathscr{S}_1 &= \left(\frac{(\Pi u^n - u^n) - (\Pi u^{n-1} - u^{n-1})}{\Delta t}, \Pi e_u^n\right)\\ &\le \frac{1}{\Delta t} \parallel \Pi e_u^n \parallel_{L^2(\Omega)} \int_{t^{n-1}}^{t^n} \parallel \partial_t(\Pi u - u) \parallel_{L^2(\Omega)} dt\\ &\le C \parallel \Pi e_u^n \parallel^2_{L^2(\Omega)} + \frac{C}{\Delta t} \parallel \partial_t(\Pi u - u) \parallel^2_{L^2(J^n;L^2(\Omega))},\end{aligned}$$

and

$$\begin{aligned}\mathscr{S}_2 &= \left(\frac{(\Pi u^{n-1} - u^{n-1}) - (\Pi \check{u}^{n-1} - \check{u}^{n-1})}{\Delta t}, \Pi e_u^n\right)\\ &\le C \parallel \Pi e_u^n \parallel^2_{L^2(\Omega)} + C \parallel \nabla(\Pi u^{n-1} - u^{n-1}) \parallel^2_{L^2(\Omega)},\end{aligned}$$

follow from Cauchy–Schwarz's inequality, Young's inequality and Lemma 10. Substituting $\mathscr{B}_1, \mathscr{B}_2, \mathscr{B}_3$ into (4.15), the desired result is reached.

4.2.2 The Right-Hand Side Term

In this subsection, we use the general analytic methods to get the bound of the right side term of (4.7).

Theorem 12 *Let u be sufficiently smooth solution of (3.1). $(\Pi u^n, \boldsymbol{\Pi}\boldsymbol{\sigma}^n, \boldsymbol{\Pi}\boldsymbol{p}^n)$ are standard L^2-projection operators of $(u^n, \boldsymbol{\sigma}^n, \boldsymbol{p}^n)$, and $(u_h^n, \boldsymbol{\sigma}_h^n, \boldsymbol{p}_h^n)$ solve (3.5). If $\boldsymbol{b} \in L^\infty(J; W^{1,\infty}(\Omega)^2)$, we have*

$$\begin{aligned}&\left|\mathscr{A}\left(\Pi u^n - u^n, \boldsymbol{\Pi}\boldsymbol{\sigma}^n - \boldsymbol{\sigma}^n, \boldsymbol{\Pi}\boldsymbol{p}^n - \boldsymbol{p}^n; \Pi e_u^n, -\boldsymbol{\Pi}\boldsymbol{e}_{\boldsymbol{p}}^n, \boldsymbol{\Pi}\boldsymbol{e}_{\boldsymbol{\sigma}}^n\right)\right|\\ &\le C\varepsilon_{\alpha_1} \int_c^d \parallel \Pi e_{p_x}^n(\cdot, y) \parallel^2_{J^{-\alpha_1/2}_{R,0}(a,b)} dy + \left(\frac{C}{\varepsilon_1} + C\varepsilon_1\right) h^{2k+1} + \frac{C}{\varepsilon_{\alpha_1}} h^{2k+2}\\ &\quad + C\varepsilon_{\alpha_2} \int_a^b \parallel \Pi e_{p_y}^n(x, \cdot) \parallel^2_{J^{-\alpha_2/2}_{R,0}(c,d)} dx + \left(\frac{C}{\varepsilon_2} + C\varepsilon_2\right) h^{2k+1} + \frac{C}{\varepsilon_{\alpha_2}} h^{2k+2}\\ &\quad + \frac{\varepsilon_1}{2} \sum_{e\in\mathscr{E}_h^B} \parallel [\![\Pi e_u^n]\!] \parallel^2_{L^2(e)} + \frac{\varepsilon_2}{2} \sum_{e\in\mathscr{E}_h^i} \parallel [\![\boldsymbol{\Pi}\boldsymbol{e}_{\boldsymbol{\sigma}}^n]\!] \parallel^2_{L^2(e)}.\end{aligned} \tag{4.16}$$

Proof From the definition of $\mathscr{A}$, we have

$$\begin{aligned}&\mathscr{A}\left(\Pi u^n - u^n, \boldsymbol{\Pi}\boldsymbol{\sigma}^n - \boldsymbol{\sigma}^n, \boldsymbol{\Pi}\boldsymbol{p}^n - \boldsymbol{p}^n; \Pi e_u^n, -\boldsymbol{\Pi}\boldsymbol{e}_{\boldsymbol{p}}^n, \boldsymbol{\Pi}\boldsymbol{e}_{\boldsymbol{\sigma}}^n\right)\\ &\le \left|\mathbb{a}(\boldsymbol{\Pi}\boldsymbol{\sigma}^n - \boldsymbol{\sigma}^n, \Pi e_u^n)\right| + \left|\mathbb{c}(I_{\boldsymbol{x}}^{\tilde{\alpha}}(\boldsymbol{\Pi}\boldsymbol{p}^n - \boldsymbol{p}^n), \boldsymbol{\Pi}\boldsymbol{e}_{\boldsymbol{p}}^n)\right|\\ &\quad + \left|\mathbb{a}(\boldsymbol{\Pi}\boldsymbol{e}_{\boldsymbol{\sigma}}^n, \Pi u^n - u^n)\right| + \left|\mathbb{d}(\Pi u^n - u^n, \Pi e_u^n)\right|\\ &\quad + \left|\mathbb{e}(\boldsymbol{\Pi}\boldsymbol{\sigma}^n - \boldsymbol{\sigma}^n, \boldsymbol{\Pi}\boldsymbol{e}_{\boldsymbol{\sigma}}^n)\right| + \left|\mathbb{c}(\boldsymbol{\Pi}\boldsymbol{\sigma}^n - \boldsymbol{\sigma}^n, -\boldsymbol{\Pi}\boldsymbol{e}_{\boldsymbol{p}}^n)\right|\\ &\quad + \left|\mathbb{c}(\boldsymbol{\Pi}\boldsymbol{p}^n - \boldsymbol{p}^n, \boldsymbol{\Pi}\boldsymbol{e}_{\boldsymbol{\sigma}}^n)\right|\\ &= \sum_{i=1}^{7} T_i.\end{aligned} \tag{4.17}$$

Using Hölder's, Young's inequalities and Lemma 8, we obtain

$$\begin{aligned}
T_1 &= \left|\mathbb{a}(\boldsymbol{\Pi\sigma}^n - \boldsymbol{\sigma}^n, \Pi e_u^n)\right| = \left|(\{\boldsymbol{\Pi\sigma}^n - \boldsymbol{\sigma}^n\}\cdot \boldsymbol{n}_e, [\![\Pi e_u^n]\!])_{\mathscr{E}_h^B}\right| \\
&\le \sum_{e\in\mathscr{E}_h^B} \| \{\boldsymbol{\Pi\sigma}^n - \boldsymbol{\sigma}^n\}\cdot \boldsymbol{n}_e \|_{L^2(e)} \| [\![\Pi e_u^n]\!] \|_{L^2(e)} \\
&\le \sum_{e\in\mathscr{E}_h^B} \left(\frac{1}{\varepsilon_1} \| \{\boldsymbol{\Pi\sigma}^n - \boldsymbol{\sigma}^n\}\cdot \boldsymbol{n}_e \|_{L^2(e)}^2 + \frac{\varepsilon_1}{4} \| [\![\Pi e_u^n]\!] \|_{L^2(e)}^2 \right) \\
&\le \frac{C}{\varepsilon_1} h^{2k+1} + \frac{\varepsilon_1}{4} \sum_{e\in\mathscr{E}_h^B} \| [\![\Pi e_u^n]\!] \|_{L^2(e)}^2 .
\end{aligned}$$

From Lemmas 1, 8, Definitions 4, 6, and Theorem 4, it follows that

$$\begin{aligned}
T_2 &= \left|\mathbb{c}(I_{\boldsymbol{x}}^{\tilde{\boldsymbol{\alpha}}}(\boldsymbol{\Pi p}^n - \boldsymbol{p}^n), \boldsymbol{\Pi e}_{\boldsymbol{p}}^n)\right| \\
&= \left|(\Pi p_x^n - p_x^n, {}_xI_b^{\alpha_1}\Pi e_{p_x}^n) + (\Pi p_y^n - p_y^n, {}_yI_d^{\alpha_2}\Pi e_{p_y}^n)\right| \\
&\le \| \Pi p_x^n - p_x^n \|_{L^2(\Omega)} \left(\int_c^d \| \Pi e_{p_x}^n(\cdot, y) \|_{J_{R,0}^{-\alpha_1}(a,b)}^2 \, dy \right)^{\frac{1}{2}} \\
&\quad + \| \Pi p_y^n - p_y^n \|_{L^2(\Omega)} \left(\int_a^b \| \Pi e_{p_y}^n(x, \cdot) \|_{J_{R,0}^{-\alpha_2}(c,d)}^2 \, dx \right)^{\frac{1}{2}} \\
&\le C \| \Pi p_x^n - p_x^n \|_{L^2(\Omega)} \left(\int_c^d \| \Pi e_{p_x}^n(\cdot, y) \|_{J_{R,0}^{-\alpha_1/2}(a,b)}^2 \, dy \right)^{\frac{1}{2}} \\
&\quad + C \| \Pi p_y^n - p_y^n \|_{L^2(\Omega)} \left(\int_a^b \| \Pi e_{p_y}^n(x, \cdot) \|_{J_{R,0}^{-\alpha_2/2}(c,d)}^2 \, dx \right)^{\frac{1}{2}} \\
&\le \frac{C}{\varepsilon_{\alpha_1}} h^{2k+2} + C\varepsilon_{\alpha_1} \int_c^d \| \Pi e_{p_x}^n(\cdot, y) \|_{J_{R,0}^{-\alpha_1/2}(a,b)}^2 \, dy \\
&\quad + \frac{C}{\varepsilon_{\alpha_2}} h^{2k+2} + C\varepsilon_{\alpha_2} \int_a^b \| \Pi e_{p_y}^n(x, \cdot) \|_{J_{R,0}^{-\alpha_2/2}(c,d)}^2 \, dx,
\end{aligned}$$

where ε_{α_1} and ε_{α_2} are chosen as sufficiently small numbers such that $C\varepsilon_{\alpha_1} \le \cos(\alpha_1\pi/2)$ and $C\varepsilon_{\alpha_2} \le \cos(\alpha_2\pi/2)$.

Integrating the first term of $\mathbb{a}(\boldsymbol{\Pi e}_{\boldsymbol{\sigma}}^n, \Pi u^n - u^n)$ by parts, and using the orthogonal property of projection operator $\boldsymbol{\Pi}$, we get

$$\begin{aligned}
T_3 &= \left|\mathbb{a}(\boldsymbol{\Pi e}_{\boldsymbol{\sigma}}^n, \Pi u^n - u^n)\right| \\
&= \left| \left(\boldsymbol{\Pi e}_{\boldsymbol{\sigma}}^n, \nabla(\Pi u^n - u^n)\right) - \left(\{\boldsymbol{\Pi e}_{\boldsymbol{\sigma}}^n\}\cdot \boldsymbol{n}_e, [\![\Pi u^n - u^n]\!]\right)_{\mathscr{E}_h^B} \right| \\
&= \left| \left([\![\boldsymbol{\Pi e}_{\boldsymbol{\sigma}}^n]\!], \{\Pi u^n - u^n\}\boldsymbol{n}_e\right)_{\mathscr{E}_h^i} \right| \\
&\le \sum_{e\in\mathscr{E}_h^i} \| [\![\boldsymbol{\Pi e}_{\boldsymbol{\sigma}}^n]\!] \|_{L^2(e)} \| \{\Pi u^n - u^n\}\boldsymbol{n}_e \|_{L^2(e)} \\
&\le \sum_{e\in\mathscr{E}_h^i} \left(\frac{1}{\varepsilon_2} \| \{\Pi u^n - u^n\}\boldsymbol{n}_e \|_{L^2(e)}^2 + \frac{\varepsilon_2}{4} \| [\![\boldsymbol{\Pi e}_{\boldsymbol{\sigma}}^n]\!] \|_{L^2(e)}^2 \right)
\end{aligned}$$

$$\leq \frac{C}{\varepsilon_2} h^{2k+1} + \frac{\varepsilon_2}{4} \sum_{e \in \mathscr{E}_h^i} \| [\![\boldsymbol{\Pi} \boldsymbol{e}_{\boldsymbol{\sigma}}^n]\!] \|_{L^2(e)}^2 .$$

With the same deduction of T_1, there is

$$\begin{aligned} T_4 &= \left| \mathrm{d}(\Pi u^n - u^n, \Pi e_u^n) \right| \\ &\leq \varepsilon_1 \sum_{e \in \mathscr{E}_h^B} \| [\![\Pi u^n - u^n]\!] \|_{L^2(e)} \| [\![\Pi e_u^n]\!] \|_{L^2(e)} \\ &\leq \varepsilon_1 \sum_{e \in \mathscr{E}_h^B} \left(\| [\![\Pi u^n - u^n]\!] \|_{L^2(e)}^2 + \frac{1}{4} \| [\![\Pi e_u^n]\!] \|_{L^2(e)}^2 \right) \\ &\leq \varepsilon_1 C h^{2k+1} + \frac{\varepsilon_1}{4} \sum_{e \in \mathscr{E}_h^B} \| [\![\Pi e_u^n]\!] \|_{L^2(e)}^2 . \end{aligned}$$

By Lemma 8, we get

$$\begin{aligned} T_5 &= \left| \mathrm{e}(\boldsymbol{\Pi} \boldsymbol{\sigma}^n - \boldsymbol{\sigma}^n, \boldsymbol{\Pi} \boldsymbol{e}_{\boldsymbol{\sigma}}^n) \right| \\ &\leq \varepsilon_2 \sum_{e \in \mathscr{E}_h^i} \| [\![\boldsymbol{\Pi} \boldsymbol{\sigma}^n - \boldsymbol{\sigma}^n]\!] \|_{L^2(e)} \| [\![\boldsymbol{\Pi} \boldsymbol{e}_{\boldsymbol{\sigma}}^n]\!] \|_{L^2(e)} \\ &\leq \varepsilon_2 \sum_{e \in \mathscr{E}_h^i} \left(\| [\![\boldsymbol{\Pi} \boldsymbol{\sigma}^n - \boldsymbol{\sigma}^n]\!] \|_{L^2(e)}^2 + \frac{1}{4} \| [\![\boldsymbol{\Pi} \boldsymbol{e}_{\boldsymbol{\sigma}}^n]\!] \|_{L^2(e)}^2 \right) \\ &\leq C \varepsilon_2 h^{2k+1} + \frac{\varepsilon_2}{4} \sum_{e \in \mathscr{E}_h^i} \| [\![\boldsymbol{\Pi} \boldsymbol{e}_{\boldsymbol{\sigma}}^n]\!] \|_{L^2(e)}^2 . \end{aligned}$$

Note that T_6 and T_7 vanish because of the orthogonal property of the projection $\boldsymbol{\Pi}$. Substituting $T_i, i = 1, \ldots, 7$ into (4.17), the desired result is obtained.

4.2.3 Error Bounds

Assuming that the solution of (1.1) is sufficiently regular, we have the following error estimates.

Theorem 13 *Let $(u^n, \boldsymbol{\sigma}^n, \boldsymbol{p}^n)$ be the exact solution of (3.1), $(u_h^n, \boldsymbol{\sigma}_h^n, \boldsymbol{p}_h^n)$ the numerical solution of the fully discrete HDG scheme (3.5). If $\boldsymbol{b} \in L^\infty(J; W^{1,\infty}(\Omega)^2)$, for any integer $N = 1, 2, \ldots$, there is*

$$\begin{aligned} &\left\| u^N - u_h^N \right\|_{L^2(\Omega)}^2 + \Delta t \sum_{n=1}^N \left(\varepsilon_1 \sum_{e \in \mathscr{E}_h^B} \| [\![u^n - u_h^n]\!] \|_{L^2(e)}^2 + \varepsilon_2 \sum_{e \in \mathscr{E}_h^i} \| [\![\boldsymbol{\sigma}^n - \boldsymbol{\sigma}_h^n]\!] \|_{L^2(e)}^2 \right. \\ &\left. 2K_{\alpha_1} \int_c^d \| (p_x^n - p_{xh}^n)(\cdot, y) \|_{J_{R,0}^{-\alpha_1/2}(a,b)}^2 dy + 2K_{\alpha_2} \int_a^b \| (p_y^n - p_{yh}^n)(x, \cdot) \|_{J_{R,0}^{-\alpha_2/2}(c,d)}^2 dx \right) \\ &\leq C(\Delta t)^2 \sum_{n=1}^N \| \partial_{\tau\tau} u \|_{L^2(J^n; L^2(\Omega))}^2 + C \sum_{n=1}^N \| \partial_t (\Pi u - u) \|_{L^2(J^n; L^2(\Omega))}^2 \\ &\quad + C_\varepsilon h^{2k+1} + C \Delta t \sum_{n=1}^N | \Pi u^{n-1} - u^{n-1} |_{H^1(\Omega)}^2, \end{aligned} \tag{4.18}$$

where $\alpha_1 = 2-\alpha, \alpha_2 = 2-\beta$, $K_{\alpha_1} = \cos(\alpha_1\pi/2) - C\varepsilon_{\alpha_1} \geq 0$, $K_{\alpha_2} = \cos(\alpha_2\pi/2) - C\varepsilon_{\alpha_2} \geq 0$, ε_{α_1} *and* ε_{α_2} *are chosen as above,* C_ε *is dependent of* $\varepsilon_1,\ \varepsilon_2$.

Proof Substituting the results of Theorems 11 and 12 into (4.7), there is

$$\begin{aligned}
&\frac{1}{2\Delta t}\left(\| \Pi e_u^n \|^2_{L^2(\Omega)} - \| \Pi e_u^{n-1} \|^2_{L^2(\Omega)}\right) + \frac{\varepsilon_1}{2}\sum_{e\in\mathscr{E}_h^B} \| [\![\Pi e_u^n]\!] \|^2_{L^2(e)} \\
&\quad + \frac{\varepsilon_2}{2}\sum_{e\in\mathscr{E}_h^i} \| [\![\boldsymbol{\Pi e}_{\boldsymbol{\sigma}}^n]\!] \|^2_{L^2(e)} + (\cos(\alpha_1\pi/2) - C\varepsilon_{\alpha_1}) \int_c^d \|\Pi e_{p_x}^n(\cdot, y)\|^2_{J_{R,0}^{-\alpha_1/2}(a,b)} dy \\
&\quad + (\cos(\alpha_2\pi/2) - C\varepsilon_{\alpha_2}) \int_a^b \|\Pi e_{p_y}^n(x, \cdot)\|^2_{J_{R,0}^{-\alpha_2/2}(c,d)} dx \\
&\leq C \| \Pi e_u^{n-1} \|^2_{L^2(\Omega)} + C \| \Pi e_u^n \|^2_{L^2(\Omega)} + C\Delta t \| \partial_{\tau\tau} u \|^2_{L^2(J^n;L^2(\Omega))} \\
&\quad + \frac{C}{\Delta t}\|\partial_t(\Pi u - u)\|^2_{L^2(J^n;L^2(\Omega))} + C \mid \Pi u^{n-1} - u^{n-1} \mid^2_{H^1(\Omega)} + C_\varepsilon h^{2k+1}.
\end{aligned}$$

With $\Pi e_u^0 = 0$, multiplying the above inequality by $2\Delta t$ on both sides, summing over n from 1 to N, and using the discrete Grönwall inequality, there is

$$\begin{aligned}
&\| \Pi e_u^N \|^2_{L^2(\Omega)} + \Delta t \sum_{n=1}^N \left(\varepsilon_1 \sum_{e\in\mathscr{E}_h^B} \| [\![\Pi e_u^n]\!] \|^2_{L^2(e)} + \varepsilon_2 \sum_{e\in\mathscr{E}_h^i} \| [\![\boldsymbol{\Pi e}_{\boldsymbol{\sigma}}^n]\!] \|^2_{L^2(e)} \right) \\
&\quad + 2\Delta t \sum_{n=1}^N (cos(\alpha_1\pi/2) - C\varepsilon_{\alpha_1}) \int_c^d \| \Pi e_{p_x}^n(\cdot, y) \|^2_{J_{R,0}^{-\alpha_1/2}(a,b)} dy \\
&\quad + 2\Delta t \sum_{n=1}^N (cos(\alpha_2\pi/2) - C\varepsilon_{\alpha_2}) \int_a^b \|\Pi e_{p_y}^n(x, \cdot)\|^2_{J_{R,0}^{-\alpha_2/2}(c,d)} dx \\
&\leq C(\Delta t)^2 \sum_{n=1}^N \|\partial_{\tau\tau} u\|^2_{L^2(J^n;L^2(\Omega))} + C \sum_{n=1}^N \|\partial_t(\Pi u - u)\|^2_{L^2(J^n;L^2(\Omega))} \\
&\quad + C\Delta t \sum_{n=1}^N \mid \Pi u^{n-1} - u^{n-1} \mid^2_{H^1(\Omega)} + C_\varepsilon h^{2k+1}.
\end{aligned}$$

By the triangle inequality, we obtain the desired result.

5 Numerical Experiment

In this section, we illustrate the numerical performance of the proposed schemes by the numerical simulations of two examples. In the first example, we take the vector function $\boldsymbol{b} = \mathbf{0}$ and verify the accuracy of the schemes with the exact smooth solution u combining with the left fractional Riemann–Liouville derivatives with respect to x-variable and y-variable, respectively. When we compute the fractional integral part in triangular meshes (see Figs. 1, 2), the Gauss points and weights are used to deal with the terms relating with the fractional operators element-by-element (see [14,26]). Since this part needs more time and memory spaces (see [22]), we only use the piecewise linear basis functions to simulate the solution

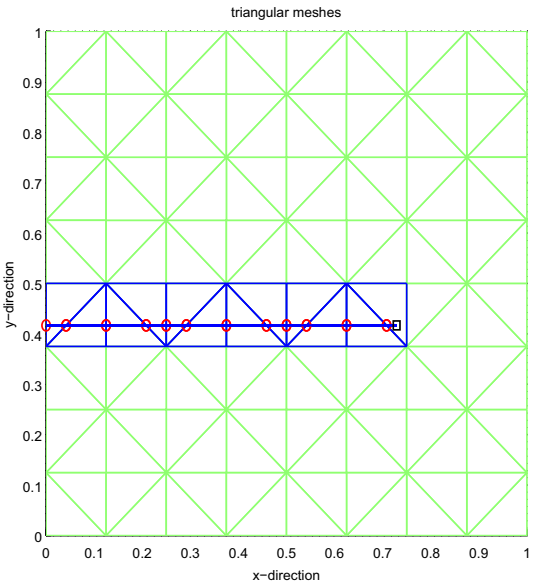

Fig. 1 All triangles in x-direction affected by the Gauss points (denoted by *black square*)

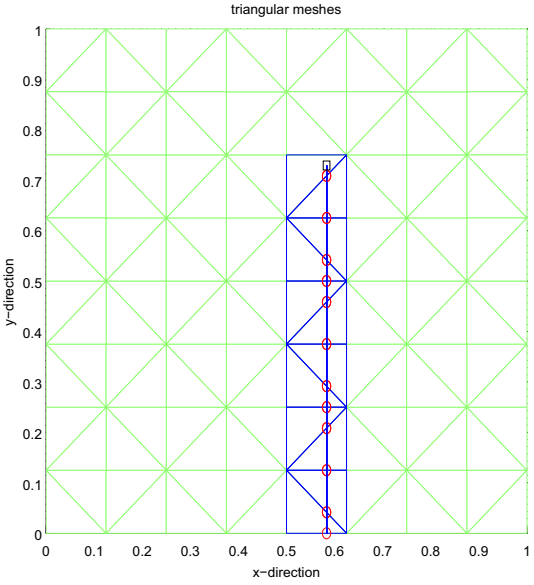

Fig. 2 All triangles in y-direction affected by the Gauss points (denoted by *black square*)

in triangular meshes. Tables 1, 2 and 3 illustrate that the schemes have a good convergence order with piecewise linear basis function for different choices of the fluxes. In the second example, we take $\boldsymbol{b}$ to be a vector function and perform some numerical experiments with some figures (see Figs. 3, 4) which justify that the schemes simulate the solution very well for 2D-fractional convection–diffusion problems.

Table 1 The L^2, L^1-errors and convergence rates for u and u_x, u_y for Example 5.1

h	$\|e_u(t)\|_{L^2}$	*Rate*	$\|e_u(t)\|_{L^1}$	*Rate*	$\|\partial_x e_u(t)\|_{L^2}$	*Rate*	$\|\partial_y e_u(t)\|_{L^2}$
$t = 0.1$, $(\alpha, \beta) = (1.2, 1.4)$, $(\varepsilon_1, \varepsilon_2) = (\mathcal{O}(1), \mathcal{O}(1))$							
1/6	1.3993e−04	–	1.0771e−04	–	1.4273e−03	–	6.4132e−03
1/10	5.6088e−05	1.79	4.1112e−05	1.89	7.2047e−03	1.34	6.8133e−03
1/14	2.9803e−05	1.88	2.1713e−05	1.90	4.8274e−04	1.19	6.9191e−03
1/18	1.8452e−05	1.91	1.3226e−05	1.97	3.4904e−04	1.29	6.9660e−03
$t = 0.1$, $(\alpha, \beta) = (1.5, 1.5)$, $(\varepsilon_1, \varepsilon_2) = (\mathcal{O}(1), \mathcal{O}(1))$							
1/6	1.8283e−04	–	1.4041e−04	–	1.1688e−03	–	6.4118e−03
1/10	7.5004e−05	1.74	5.6669e−05	1.78	5.1740e−04	1.60	6.7972e−03
1/14	4.0967e−05	1.80	3.1156e−05	1.78	3.2141e−04	1.41	6.9127e−03
1/18	2.5475e−05	1.89	1.9258e−05	1.91	2.2281e−04	1.46	6.9610e−03
$t = 0.1$, $(\alpha, \beta) = (1.9, 1.6)$, $(\varepsilon_1, \varepsilon_2) = (\mathcal{O}(1), \mathcal{O}(1))$							
1/6	2.6485e−04	–	1.9290e−04	–	1.1859e−03	–	6.4542e−03
1/10	1.1544e−04	1.63	8.6542e−05	1.57	5.3599e−04	1.56	6.7608e−03
1/14	6.7712e−05	1.59	5.0400e−05	1.61	3.3163e−04	1.43	6.8829e−03
1/18	4.5463e−05	1.59	3.3857e−05	1.58	2.3476e−04	1.38	6.9387e−03

Table 2 The L^2, L^1-errors and convergence rates for u and u_x, u_y for Example 5.1

h	$\|e_u(t)\|_{L^2}$	*Rate*	$\|e_u(t)\|_{L^1}$	*Rate*	$\|\partial_x e_u(t)\|_{L^2}$	*Rate*	$\|\partial_y e_u(t)\|_{L^2}$
$t = 1$, $(\alpha, \beta) = (1.2, 1.4)$, $(\varepsilon_1, \varepsilon_2) = (\mathcal{O}(1), \mathcal{O}(1))$							
1/6	8.2881e−05	–	7.2374e−05	–	4.7733e−04	–	2.5556e−03
1/10	3.2222e−05	1.85	2.7700e−05	1.88	2.6204e−04	1.17	2.7560e−03
1/14	1.6162e−05	2.05	1.3515e−05	2.13	1.7748e−04	1.06	2.8077e−03
1/18	9.9448e−06	1.93	8.2787e−06	1.95	1.3085e−04	1.21	2.8291e−03
$t = 1$, $(\alpha, \beta) = (1.5, 1.5)$, $(\varepsilon_1, \varepsilon_2) = (\mathcal{O}(1), \mathcal{O}(1))$							
1/6	8.7928e−05	–	7.4712e−05	–	4.1510e−04	–	2.5466e−03
1/10	3.5668e−05	1.77	2.9706e−05	1.81	1.9555e−04	1.47	2.7408e−03
1/14	1.8524e−05	1.95	1.4885e−05	2.05	1.2291e−04	1.38	2.8010e−03
1/18	1.1432e−05	1.92	9.0662e−06	1.97	8.6553e−05	1.40	2.8244e−03
$t = 1$, $(\alpha, \beta) = (1.9, 1.6)$, $(\varepsilon_1, \varepsilon_2) = (\mathcal{O}(1), \mathcal{O}(1))$							
1/6	1.1250e−04	–	8.4393e−05	–	4.6409e−04	–	2.5983e−03
1/10	4.7998e−05	1.67	3.6510e−05	1.64	2.1614e−04	1.50	2.7410e−03
1/14	2.7916e−05	1.61	2.0971e−05	1.65	1.3512e−04	1.40	2.7985e−03
1/18	1.8767e−05	1.58	1.4104e−05	1.58	9.5762e−05	1.37	2.8216e−03

Example 5.1 Consider 2D space-fractional convection–diffusion problem (1.1) in domain $\Omega = (0, 1) \times (0, 1)$. The initial condition and the exact solution are specified as

$$\begin{cases} u(x, y, t) = e^{-t} x^2 (x-1)^2 y^2 (y-1)^2, \\ u_0(x, y) = x^2 (x-1)^2 y^2 (y-1)^2, \\ \boldsymbol{b}(x, y, t) = (0, 0). \end{cases} \tag{5.1}$$

Table 3 The L^2, L^1-errors and convergence rates for u and u_x, u_y for Example 5.1

h	$\|e_u(t)\|_{L^2}$	*Rate*	$\|e_u(t)\|_{L^1}$	*Rate*	$\|\partial_x e_u(t)\|_{L^2}$	*Rate*	$\|\partial_y e_u(t)\|_{L^2}$
$t = 1, (\alpha, \beta) = (1.9, 1.6), (\varepsilon_1, \varepsilon_2) = (\mathcal{O}(h^{-1}), \mathcal{O}(1))$							
1/6	5.2142e−05	–	4.1592e−05	–	4.0695e−04	–	2.5777e−03
1/10	1.9772e−05	1.90	1.5784e−05	1.90	1.7761e−04	1.62	2.7383e−03
1/14	9.5805e−06	2.15	7.5267e−06	2.20	1.1392e−04	1.32	2.7976e−03
1/18	5.8213e−06	1.98	4.6596e−06	1.91	7.8388e−05	1.49	2.8210e−03
$t = 1, (\alpha, \beta) = (1.9, 1.6), (\varepsilon_1, \varepsilon_2) = (\mathcal{O}(h^{-1}), \mathcal{O}(h))$							
1/6	4.8702e−05	–	3.9358e−05	–	4.2857e−04	–	2.5666e−03
1/10	1.9169e−05	1.83	1.5766e−05	1.79	1.9937e−04	1.50	2.7356e−03
1/14	9.2520e−06	2.17	7.6271e−06	2.16	1.2817e−04	1.31	2.7962e−03
1/18	5.6525e−06	1.96	4.6650e−06	1.96	8.9725e−05	1.42	2.8202e−03
$t = 1, (\alpha, \beta) = (1.9, 1.6), (\varepsilon_1, \varepsilon_2) = (\mathcal{O}(1), \mathcal{O}(h))$							
1/6	8.6286e−05	–	6.6645e−05	–	4.5649e−04	–	2.5761e−03
1/10	3.4635e−05	1.79	2.8021e−05	1.70	2.0660e−04	1.55	2.7365e−03
1/14	1.7787e−05	1.98	1.4393e−05	1.98	1.2993e−04	1.38	2.7964e−03
1/18	1.0969e−05	1.92	8.9170e−06	1.91	8.9646e−05	1.48	2.8200e−03

Then the force term f is determined accordingly from (1.1). In this case, we present a few results to numerically validate the analysis.

For the numerical simulations, in order to validate the stability and the accuracy of the presented HDG scheme, we choose the time-stepsize, $\Delta t = \mathcal{O}(h^{3/2})$, used to advance the discrete formulation from t^{n-1} to t^n, $n = 1, 2, \ldots, N$. The experimental convergence rate is given by

$$rate = \frac{\log\left(\| u(t) - u_{h_1}(t) \|_{L^2(\mathscr{E}_{h_1})} \,/\, \| u(t) - u_{h_2}(t) \|_{L^2(\mathscr{E}_{h_2})}\right)}{\log(h_1/h_2)}.$$

In Tables 1 and 2 we choose different observation time $t = 0.1, 1$ and α, β to justify that the convergence rates at least have an order of $\mathcal{O}(h^{3/2})$ for the solution u in L^2, L^1-norms based on the piecewise linear basis function. In Table 3 we take the same choice of ε_1, ε_2 as Ref. [3] and see that the convergence rates increase to $\mathcal{O}(h^2)$ (see the explanations in Ref. [3]). Comparing the numerical results with the work [26], we can see that the HDG method has smaller numerical errors for the first order polynomial approximation.

Example 5.2 In this example, we investigate the approximation solution of problem (1.1). For convenience, we still choose the domain $\Omega = (0, 1) \times (0, 1)$. The exact solution u, initial value and the vector function $\boldsymbol{b}$ are given by

$$\begin{cases} u(x, y, t) = e^{-t} x^2 (x - 0.5)^2 (x - 1)^2 y^2 (y - 0.5)^2 (y - 1)^2, \\ u_0(x, y) = x^2 (x - 0.5)^2 (x - 1)^2 y^2 (y - 0.5)^2 (y - 1)^2, \\ \boldsymbol{b} = ((x - 0.5), -(y - 0.5)). \end{cases} \tag{5.2}$$

For the second example, in order to further support the theoretical convergence and justify the powerful HDG scheme, we take $\boldsymbol{b}$ to be nonzero vector function and give some approximation

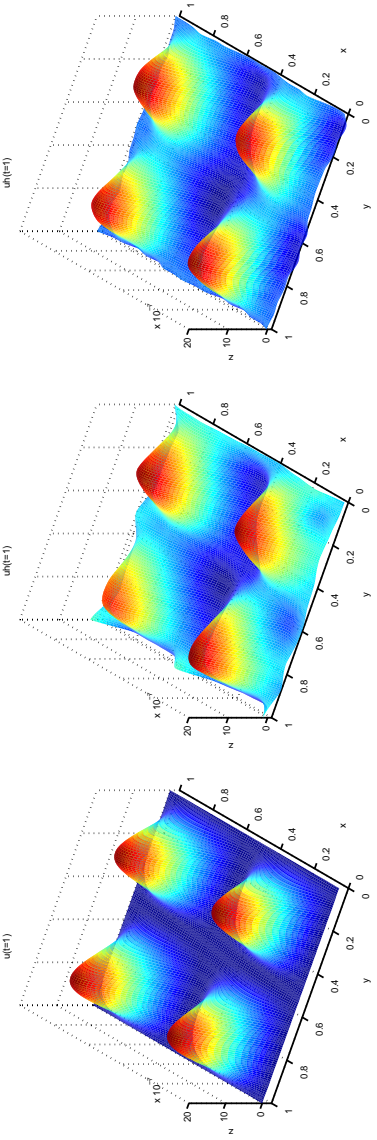

Fig. 3 Exact solution u and the numerical solutions u_h at $t = 1$ for Example 5.2

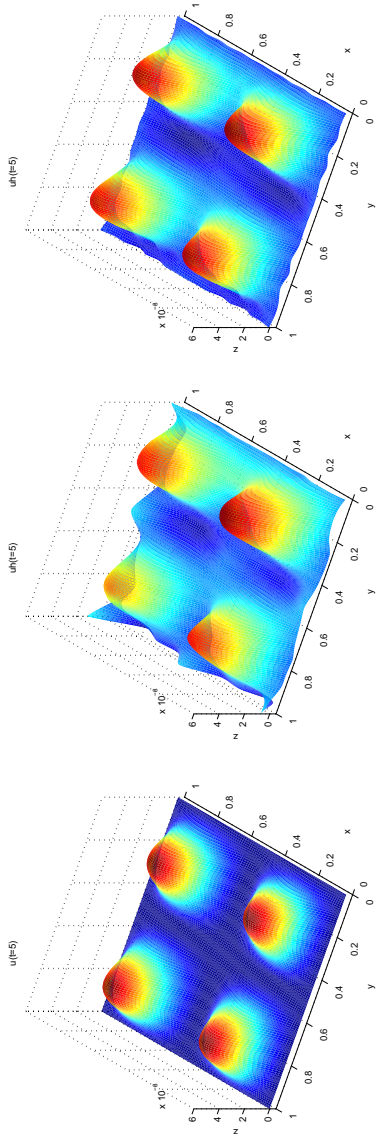

(a) **(b)** **(c)**

Fig. 4 Exact solution u and the numerical solutions u_h at $t = 5$ for Example 5.2

solutions with the refining space-step h to compare with the exact solutions and display the efficiency of the simulations.

Figure 3 displays the exact solution u and the numerical solutions u_h based on different space stepsizes $h = \frac{1}{8}, \frac{1}{16}$ at $t = 1$ with $\alpha = 1.2$, $\beta = 1.4$, $\varepsilon_1 = \varepsilon_2 = 1$. Figure 4 displays the exact solution u and the numerical solutions u_h based on different space stepsizes $h = \frac{1}{8}, \frac{1}{16}$ at $t = 5$ with $\alpha = 1.9$, $\beta = 1.6$, $\varepsilon_1 = h^{-1}$, $\varepsilon_2 = 1$. It is clear that the exact solution of Example 5.2 is nonnegative with four hills. In the simulations, the P^1-HDG solutions recover the exact solution perfectly with all four hills in coarse meshes. Note that the numerical results display that the approximations are more and more accurate with the refining of the meshes.

6 Conclusions

By carefully introducing the auxiliary variables, constructing the numerical fluxes, adding the penalty terms, and using the characteristic method to deal with the time derivative and convective term, we design the effective HDG schemes to solve 2D space-fractional convection–diffusion equations with triangular meshes. As we know, this work is the first time to deal two-dimensional space-fractional convection–diffusion equation with triangular mesh by the DG method. The stability and error bounds analysis are investigated.

Besides the general advantages of HDG method, the presented scheme is shown to have the following benefits: (1) it is symmetric, so easy to deal with the fractional operators; (2) theoretically, the stability can be more easily proved; (3) the penalty terms make the error analysis more convenient; (4) numerically verified to have efficient approximations; (5) the schemes are performed very well in triangular meshes; (6) it is possible to use this scheme to solve nonlinear equations which is the future research task.

Acknowledgments This work was partially supported by the National Basic Research (973) Program of China under Grant 2011CB706903, the National Natural Science Foundation of China under Grant 11271173 and 11471150, and the CAPES and CNPq in Brazil.

References

1. Benson, D.A., Wheatcraft, S.W., Meerschaert, M.M.: The fractional-order governing equation of Lévy motion. Water Resour. Res. **36**(6), 1413–1423 (2000)
2. Carreras, B.A., Lynch, V.E., Zaslavsky, G.M.: Anomalous diffusion and exit time distribution of particle tracers in plasma turbulence model. Phys. Plasmas **8**(12), 5096–5103 (2001)
3. Castilo, P., Cockburn, B., Perugia, I., Sötzau, D.: An a priori error analysis of the local discontinuous Galerkin method for elliptic problems. SIAM J. Numer. Anal. **38**(5), 1676–1706 (2000)
4. Chen, Z.X.: Characteristic mixed discontinuous finite element methods for advection-dominated diffusion problems. Comput. Methods Appl. Mech. Eng. **191**, 2509–2538 (2002)
5. Chen, Z.X., Ewing, R.E., Jiang, Q.Y., Spagnuolo, M.: Error analysis for characteristic-based methods for degenerate parabolic problems. SIAM J. Numer. Anal. **40**, 1491–1515 (2003)
6. Chen, M.H., Deng, W.H.: A second-order numerical method for two-dimensional two-sided space fractional convection-diffusion equation. Appl. Math. Model. **38**(13), 3244–3259 (2014)
7. Cockburn, B., Shu, C.-W.: The local discontinuous Galerkin method for time-dependent convection–diffusion systems. SIAM J. Numer. Anal. **35**(6), 2440–2463 (1998)
8. Cockburn, B., Shu, C.-W.: Runge–Kutta discontinuous Galerkin methods for convection-dominated problems. J. Sci. Comput. **16**(3), 173–261 (2001)
9. Cockburn, B., Mustapha, K.: A hybridizable discontinuous Galerkin method for fractional diffusion problems. Numer. Math. **130**(2), 293–314 (2015)

10. Cui, M.R.: A high-order compact exponential scheme for fractional convection–diffusion equations. J. Comput. Appl. Math. **255**, 404–416 (2014)
11. Deng, W.H., Hesthaven, J.S.: Local discontinuous Galerkin methods for fractional diffusion equations. ESAIM Math. Model. Numer. Anal. **47**, 1845–1864 (2013)
12. Douglas Jr, J., Russell, T.F.: Numerical method for convection-dominated diffusion problems based on combining the method of characteristics with finite element or finite difference procedures. SIAM J. Numer. Anal. **19**(5), 871–885 (1982)
13. Ervin, V.J., Roop, J.P.: Variational formulation for the stational fractional advection dispersion equation. Numer. Methods Partial Differ. Equ. **22**(3), 558–576 (2006)
14. Hesthaven, J.S., Warburton, T.: Nodal Discontinuous Galerkin Methods: Algorithms, Analysis, and Applications. Springer, New York (2008)
15. Ji, X., Tang, H.Z.: High-order accurate Runge–Kutta (local) discontinuous Galerkin methods for one- and two-dimensional fractional diffusion equations. Numer. Math. Theor. Methods Appl. **5**(3), 333–358 (2012)
16. Kirchner, J.W., Feng, X.H., Neal, C.: Fractal stream chemistry and its implication for contaminant transport in catchments. Nature **403**, 524–526 (2002)
17. Lin, Y., Xu, C.J.: Finite difference/spectral approximations for the time-fractional diffusion equations. J. Comput. Phys. **225**, 1533–1552 (2007)
18. Liu, F., Zhuang, P., Anh, V., Turner, I., Burrage, K.: Stability and convergence of the difference methods for the space–time fractional advection–diffusion equation. Appl. Math. Comput. **191**, 12–20 (2007)
19. Magin, R.L.: Fractional Calculus in Bioengineering. Begell House, Redding (2006)
20. Mclean, W., Mustapha, K.: Convergence analysis of a discontinuous Galerkin method for a sub-diffusion equation. Numer. Algor. **52**(1), 69–88 (2009)
21. Mclean, W., Mustapha, K.: Superconvergence of a discontinuous Galerkin method for fractional diffusion and wave equations. SIAM J. Numer. Anal. **51**(1), 491–515 (2013)
22. Mclean, W.: Fast summation by interval clustering for an evolution equation with memory. SIAM J. Sci. Comput. **34**(6), A3039–A3056 (2012)
23. Mustapha, K., Mclean, W.: Piece-linear, discontinuous Galerkin method for a fractional diffusion equation. Numer. Algor. **56**(2), 159–184 (2001)
24. Mustapha, K.: Time-stepping discontinuous Galerkin methods for fractional diffusion problems. Numer. Math. **130**(3), 497–516 (2015)
25. Oldham, K.B., Spanier, J.: The Fractional Calculus. Academic Press, New York (1974)
26. Qiu, L.L., Deng, W.H., Hesthaven, J.S.: Nodal discontinuous Galerkin methods for fractional diffusion equations on 2D domain with triangualr meshes. J. Comput. Phys. **298**, 678–694 (2015)
27. Rivière, B.: Discontinuous Galerkin Methods for Solving Elliptic and Parabolic Equations: Theory and Implementation. SIAM, Philadelphia (2008)
28. Shlesinger, M.F., West, B.J., Klafter, J.: Lévy dynamics of enhanced diffusion: application to turbulence. Phys. Rev. Lett. **58**(11), 1100–1103 (1987)
29. Wang, Z.B., Vong, S.W.: A high-order exponential ADI scheme for two dimensional time fractional convection–diffusion equations. Comput. Math. Appl. **68**, 185–196 (2014)
30. Xu, Q., Hesthaven, J.S.: Discontinuous Galerkin method for fractional convection–diffusion equations. SIAM J. Numer. Anal. **52**(1), 405–423 (2014)
31. Zhai, S.Y., Feng, X.L., He, Y.N.: An unconditionally stable compact ADI method for three-dimensional time-fractional convection–diffusion equations. J. Comput. Phys. **269**, 138–155 (2014)